Published in final edited form as:
Neuron. 2013 July 24; 79(2): 322–334. doi:10.1016/j.neuron.2013.05.012.

Intersecting Circuits Generate Precisely Patterned Retinal Waves

Alejandro Akrouh[1,2] and **Daniel Kerschensteiner**[1,3,4,*]

[1]Department of Ophthalmology and Visual Sciences, Washington University School of Medicine, 660 S. Euclid Avenue, Saint Louis, MO 63110, USA

[2]Graduate Program in Neuroscience, Washington University School of Medicine, 660 S. Euclid Avenue, Saint Louis, MO 63110, USA

[3]Department of Anatomy and Neurobiology, Washington University School of Medicine, 660 S. Euclid Avenue, Saint Louis, MO 63110, USA

[4]Hope Center for Neurological Disorders, Washington University School of Medicine, 660 S. Euclid Avenue, Saint Louis, MO 63110, USA

SUMMARY

The developing retina generates spontaneous glutamatergic (stage III) waves of activity that sequentially recruit neighboring ganglion cells with opposite light responses (ON and OFF RGCs). This activity pattern is thought to help establish parallel ON and OFF pathways in downstream visual areas. The circuits that produce stage III waves and desynchronize ON and OFF RGC firing remain obscure. Using dual patch clamp recordings, we find that ON and OFF RGCs receive sequential excitatory input from ON and OFF cone bipolar cells (CBCs), respectively. This input sequence is generated by crossover circuits, in which ON CBCs control glutamate release from OFF CBCs via diffusely stratified inhibitory amacrine cells. In addition, neighboring ON CBCs communicate directly and indirectly through lateral glutamatergic transmission and gap junctions, both of which are required for wave initiation and propagation. Thus, intersecting lateral excitatory and vertical inhibitory circuits give rise to precisely patterned stage III retinal waves.

INTRODUCTION

Spontaneous neuronal activity pervades the developing nervous system and correlations contained in its patterns guide the synaptic refinement of many immature circuits (Blankenship and Feller, 2010; Katz and Shatz, 1996). This has best been studied in the developing visual system, where waves of spontaneous activity originate in the retina (Meister et al., 1991) and dictate firing patterns up to primary visual cortex (V1) (Ackman et al., 2012; Mooney et al., 1996). Across many species, retinal waves mature in three stereotypic stages (I-III) (Blankenship and Feller, 2010; Wong, 1999). In each stage, distinct

*Correspondence: dkerschensteiner@wustl.edu.

AUTHOR CONTRIBUTIONS

A.A. and D.K. planned and performed the experiments, analyzed the data, and wrote the manuscript.

mechanisms give rise to unique activity patterns that serve specific functions in organizing visual circuits.

During stage III (postnatal day 10 – 14, P10–14 mice), the firing patterns of different RGC types diverge (Lee et al., 2002; Liets et al., 2003; Wong and Oakley, 1996). In particular, we recently discovered that within each stage III wave neighboring RGCs with opposite light responses fire asynchronous bursts of action potentials in a fixed order: ON before OFF (Kerschensteiner and Wong, 2008). Multiple lines of evidence indicate that this activity pattern is critical for the segregation of ON and OFF retinogeniculate projections. First, ON/OFF segregation in the dorsolateral geniculate nucleus (dLGN) emerges concurrent with stage III waves (Hahm et al., 1991; Morgan and Thompson, 1993). Second, blockade of retinal activity or its transmission to dLGN neurons during this period prevents ON/OFF segregation (Cramer and Sur, 1997; Dubin et al., 1986; Hahm et al., 1991). Third, mouse mutants with precocious stage III waves display excessive ON/OFF segregation (Chandrasekaran et al., 2007; Grubb et al., 2003). Fourth, artificial neuronal networks with burst-time dependent plasticity rules similar to those found in subcortical visual circuits (Butts et al., 2007; Shah and Crair, 2008) undergo reliable ON/OFF segregation in response to stage III wave patterns (Gjorgjieva et al., 2009). In addition to guiding refinement of dLGN circuits, the asynchronous activation of ON and OFF RGCs appears well suited to shape the emergence of ON/OFF domains and orientation selectivity in V1 (Jin et al., 2008; Miller, 1994). At the same time, distance-dependent correlations imposed by the lateral propagation of stage III waves and disjoint binocular RGC activity are needed to maintain retinotopic organization and eye-specific segregation of retinofugal projections (Chapman, 2000; Demas et al., 2006; Zhang et al., 2012).

The activation of RGCs during stage III waves is known to be mediated by glutamate receptors and a transient rise in extrasynaptic glutamate has been shown to accompany each wave (Blankenship et al., 2009; Firl et al., 2013; Wong et al., 2000). However, the circuits that initiate and laterally propagate stage III waves, and desynchronize the activity of neighboring ON and OFF RGCs remain obscure.

Here, we systematically combine dual patch clamp recordings of morphologically identified neurons in the retina to elucidate the circuits and mechanisms that give rise to the unique activity patterns of stage III waves. We find that sequential spike bursts of ON and OFF RGCs are generated by consecutive glutamate release from ON and OFF CBCs. We identify and characterize crossover circuits involving diffuse glycinergic and GABAergic amacrine cells (ACs) through which ON CBCs hyperpolarize OFF CBCs to delay glutamate release and show that glutamate uptake, mediated at least in part by Mueller glia (MGs), is required for the separation of excitatory input to ON and OFF RGCs. In addition to vertical inhibitory networks, we discover two lateral excitatory circuit mechanisms that link ON CBCs and underlie stage III wave initiation and propagation.

RESULTS

Spike trains and synaptic inputs of ON and OFF RGCs during glutamatergic waves

We began our investigation into the circuit mechanisms that generate and pattern stage III waves by obtaining dual whole-cell patch clamp recordings from RGCs in flat-mounted P11–13 retinas. To minimize distortions in the relative timing of activity introduced by lateral wave propagation, we targeted neighboring RGCs with overlapping dendritic territories (Figure 1A and 1B; overlap: 59.4 % ± 3.4 %, mean ± SEM, n = 25). Current-clamp recordings showed, in agreement with previous studies (Blankenship et al., 2011; Kerschensteiner and Wong, 2008), that stage III waves often occur in clusters with multiple bursts of activity separated by prolonged periods of silence (Figure 1C). More importantly,

these recordings confirmed our previous multielectrode-array-based observation that within each wave neighboring ON and OFF RGCs fire asynchronous bursts of action potentials in a fixed order: ON before OFF (Figure 1D and 1E, peak time of OFF-ON crosscorrelation (PT): 755 ± 134 ms, mean ± SEM, n = 11) (Kerschensteiner and Wong, 2008). The spontaneous activity of RGCs of the same response sign (i.e. ON-ON or OFF-OFF), in contrast, is synchronized (PT: 25 ± 25 ms, n = 4; $p < 0.01$ for comparison to OFF-ON).

The precise sequence of ON and OFF RGC spike bursts during glutamatergic waves could arise from distinctly timed excitatory and/or inhibitory inputs to these cells, differences in their intrinsic excitability, or combinations thereof. To begin distinguishing among these possibilities we examined synaptic inputs to RGCs during stage III waves. Voltage-clamp recordings at the reversal potential for inhibitory conductances (−60 mV) revealed sequential excitatory postsynaptic currents (EPSCs) in ON and OFF RGCs. The timing of EPSCs matched the spike patterns of these neurons during waves (Figure 1F and 1G; OFF-ON PT: Control: 698 ± 42 ms, n = 15; same sign PT: 3.5 ± 16 ms, n = 10; $p < 10^{-4}$). From here on, we will refer to the distinct periods of each wave during which ON and OFF RGCs receive excitation (and spike) as the wave's ON and OFF phases, respectively.

Unlike EPSCs, inhibitory postsynaptic currents (IPSCs) of ON and OFF RGCs recorded at the reversal potential for excitatory conductances (0 mV) were synchronized similar to those of same sign RGCs (Figure 1H and 1I; OFF-ON PT: −27 ± 36 ms, n = 7; same sign PT: −44 ± 22 ms, n = 7; $p > 0.8$).

OFF RGCs receive crossover inhibition from ON circuits during stage III waves

To determine whether RGCs receive inhibition during the ON and/or OFF phase of stage III waves, we simultaneously recorded EPSCs in ON RGCs and IPSCs in OFF RGCs (Figure 1J). The coincidence of these inputs (Figure 1K, PT: 2.6 ± 9.3 ms, n = 8) suggests that inhibition to both OFF and ON RGCs is driven by the same circuit elements that provide excitatory input to ON RGCs. As a result, ON RGCs receive simultaneous excitation and inhibition, whereas inhibition precedes excitation for OFF RGCs. In addition to differences in their timing, the relative weights of excitatory and inhibitory synaptic conductances were reversed between ON and OFF RGCs (Figure 1K *inset*; ON g_{inh}/g_{exc}: 0.67 ± 0.09, n = 25 cells; OFF g_{inh}/g_{exc}: 2.35 ± 0.26, n = 31 cells; $p < 10^{-7}$).

Because synaptic inhibition precedes excitation in OFF RGCs, postinhibitory rebound could contribute to their firing (Margolis and Detwiler, 2007). To compare the importance of rebound depolarizations to those mediated by synaptic excitation, we recorded OFF RGC responses to somatic current injections (Figure S1). Even for current steps (−150 pA) that hyperpolarized OFF RGCs (−102.6 ± 8.3 mV, n = 7 cells) well below the likely reversal potential for inhibitory conductances at this age (Zhang et al., 2006), only two of seven cells fired rebound spikes. Moreover, when observed, rebound firing gave rise to only few action potentials compared to the robust spike bursts elicited by depolarizing current injections (Figure S1) and observed during waves (Figure 1C and 1D). Responses of ON RGCs to current injections were similar to those of OFF RGCs (Figure S1).

Thus, it appears that the offset bursts of ON and OFF RGCs are elicited by sequential excitatory inputs to these neurons, which in the case of ON RGCs outweigh simultaneous inhibitory inputs and in the case of OFF RGCs are preceded by inhibition.

ON CBCs depolarize and OFF CBCs hyperpolarize during the ON phase of stage III waves

Several studies have shown that excitatory input to RGCs during stage III waves is mediated by glutamate and recent reports identify BCs as its likely source (Blankenship et al., 2009; Firl et al., 2013; Wong et al., 2000). However, how BCs themselves respond during waves is

not well understood. To address this question and elucidate the mechanisms that offset excitatory inputs to ON and OFF RGCs, we obtained dual whole-cell patch clamp recordings from BCs and RGCs with overlapping neurite territories in P11–13 retinal flat mount preparations (Figure 2A and 2B). The dendrites of BCs contact either rod (RBCs) or cone (CBCs) photoreceptors. All CBCs (43/43 cells) but no RBCs (0/4 cells) we recorded participated in stage III waves. Like RGCs, CBCs can be grouped into ON and OFF classes. The axons of ON CBCs stratify in the inner 3/5 of the IPL, those of OFF CBCs in the outer 2/5 where they contact the dendrites of ON and OFF RGCs, respectively (Ghosh et al., 2004). Simultaneous recordings of ON CBCs and ON RGCs revealed that during each stage III wave, ON CBCs depolarize while their membrane potential remains relatively stable between waves (Figure 2C; V_{Rest}: −59.4 ± 1.6 mV, n = 27). The timing and shape of ON CBC depolarizations matched those of concurrently recorded ON RGC EPSCs (Figure 2D and 2E; PT: 56 ± 43 ms, n = 18).

In contrast, OFF CBCs hyperpolarize during each stage III wave and rest at higher membrane potentials in between (Figure 2F; V_{Rest}:−48.4 ± 2.4 mV, n = 16 cells, $p < 10^{-3}$ for comparison to ON CBCs). The timing of the respective events, similar to depolarizations of ON CBCs, was aligned with the ON phase of each wave (Figure 2G, trough time of crosscorrelation: 52 ± 194 ms, n = 10). To further quantify voltage changes in ON and OFF CBCs, we algorithmically detected waves (Experimental Procedures) and subtracted from the voltage extremum during a wave its average value before and after. Voltage excursions of ON and OFF CBCs measured in this way had similar amplitudes but opposite signs (Figure 2H, ON CBCs: 13.1 ± 1 mV, n = 27; OFF CBCs: −12.6 ± 1.6 mV, n = 16, $p < 10^{-7}$). This was true irrespective of whether waves were detected based on the CBC voltage itself or on simultaneously recorded excitation to RGCs (Figure S2). To explicitly test the concurrence of CBC voltage fluctuations with stage III waves, we compared the probability with which RGC EPSCs coincided with CBC depolarizations (ON) or hyperpolarizations (OFF) in recorded traces to simulations in which the timing of CBC events was randomly shifted. In each case, the coincidence of CBC and RGC events was significantly higher in the recorded than in the randomized traces (Figure 2I, observed: 71% ± 2%, random 17% ± 1%, n = 39, $p < 10^{-7}$). Since RGC EPSCs at this age were shown to be largely restricted to waves (Blankenship et al., 2009), it follows that the CBC voltage fluctuations we discover here are as well. Events detected only in RGC or CBC traces most likely reflect waves propagating along paths that included most of the neurites of one but not the other neuron recorded.

Thus, ON CBCs excite ON RGCs as they depolarize during the ON phase of stage III waves, whereas OFF CBCs, instead of depolarizing during the OFF phase of waves, hyperpolarize during the ON phase and release glutamate onto OFF RGCs as their voltage returns to baseline.

Crossover inhibition hyperpolarizes OFF CBCs during the ON phase of stage III waves

To probe the mechanisms that hyperpolarize OFF CBCs, we carried out voltage-clamp recordings from these cells. In doing so, we observed large IPSCs in OFF CBCs that coincided with EPSCs in simultaneously recorded ON RGCs (Figure 3A and 3B; PT: 30 ± 98 ms, n = 7). Importantly, the inhibitory inputs to OFF CBCs far outweighed coinciding excitatory ones (Figures 3C and S4C; g_{inh}/gexc: 7.56 ± 1.43, n = 11).

Previous results suggest that glycine and GABA receptors mediate inhibition to OFF CBCs at this age (Schubert et al., 2008). Consistent with this, we found that while strychnine (500 nM) alone was sufficient to suppress most wave-associated OFF CBC hyperpolarizations (Figure 3D and 3E), blockade of both glycinergic and GABAergic transmission (strychnine 500 nM, gabazine 5 nM, TPMPA 50 nM) was needed to depolarize OFF CBCs during stage

III waves (Figure 3D and 3E; Control: −13.8 ± 2.1 mV; -Gly: −0.2 ± 3.1 mV; -Gly -$GABA_{A/C}$: 7.0 ± 2.7 mV, n = 6; $p < 0.03$ for all comparisons). Blockade of inhibition had no effect on the amplitude of voltage fluctuations in ON CBCs (Control: 16.1 ± 2.9 mV; -Gly -$GABA_{A/C}$: 15.5 ± 4.3 mV, n = 5; $p > 0.8$), but raised the frequency of waves in both ON and OFF CBCs (Figure S3; Control: 0.082 ± 0.008 Hz; -Gly -$GABA_{A/C}$: 0.238 ± 0.032 Hz, n = 11, $p < 10^{-3}$).

From these results, we conclude that ON CBCs drive crossover inhibition onto both OFF RGC dendrites and OFF CBC axon terminals. This inhibition involves glycinergic and GABAergic synaptic transmission, and overwhelms synchronous excitatory inputs to OFF CBCs.

Diffuse ACs likely provide crossover inhibition to OFF CBCs and OFF RGCs

To identify the cells that mediate crossover inhibition, we obtained dual recordings from ACs and RGCs during stage III waves. ACs are a morphologically diverse class of inhibitory interneurons in the inner retina (MacNeil and Masland, 1998). For our experiments, we targeted ACs with diffusely stratified neurites that are well positioned to convey signals between ON and OFF CBCs in the IPL (Figure 4A and 4B). In agreement with previous studies, we found that most diffuse ACs had narrow to medium-sized lateral fields (territory: 960 ± 227 μm^2, n = 14) (MacNeil and Masland, 1998; Menger et al., 1998). Uniformly, these ACs depolarized from rest during stage III waves (Figure 4C and 4D; V_{Rest}: −55.1 ± 3.3 mV, ΔVoltage: 14.9 ± 1.6 mV, n = 18). Simultaneous recordings of EPSCs in ON RGCs or IPSCs in OFF RGCs demonstrated that AC depolarizations occurred during the ON phase of each wave (Figure 4E and 4F; PT: 33 ± 51 ms, n = 9) and voltage-clamp recordings revealed correlated EPSCs in diffuse ACs and ON RGCs (Figure 4G and 4H; PT: 19 ± 46 ms, n = 5).

Thus, it appears that during the ON phase of stage III waves ON CBCs release glutamate and depolarize glycinergic and GABAergic diffuse ACs, which crossover inhibit OFF CBCs and OFF RGCs.

Blockade of synaptic inhibition or glutamate uptake synchronizes excitatory input to ON and OFF RGCs

If delayed excitation and bursting of OFF RGCs depend on crossover inhibition of OFF CBCs by diffuse ACs, as we suggest, then blockade of inhibition, which inverts the responses of OFF CBCs, should advance excitatory inputs and spike bursts of OFF RGCs to the ON phase of stage III waves. Voltage- and current-clamp recordings from neighboring ON and OFF RGCs in the presence of strychnine, gabazine and TPMPA showed that indeed blocking glycine, $GABA_A$ and GABAC receptors synchronized EPSCs in OFF RGCs and ON RGCs (Figure 5A and 5B; Control: 698 ± 42 ms, n = 15; -Gly -$GABA_{A/C}$: 68 ± 42 ms, n = 4, $p < 0.005$) and realigned their spike trains (Figure S5; Control: 755 ± 134 ms, n = 11; -Gly -$GABA_{A/C}$: 40 ± 68 ms, n = 5, $p < 0.005$) (Kerschensteiner and Wong, 2008).

To maintain temporal separation of the excitatory inputs to ON and OFF RGCs, the spread of extrasynaptic glutamate needs to be restricted to the distinct sublaminae in which their dendrites stratify. In support of a role for excitatory amino acid transporters (EAATs) in process, we found that EPSCs in ON and OFF RGCs were synchronized by application of TBOA (25 μM) (Figure 5C and 5D; Control: 698 ± 42 ms, n = 15; -EAAT: 31 ± 28 ms, n = 5, $p < 0.002$). Furthermore, dual patch clamp recordings from MGs and RGCs showed that MGs depolarize during each neuronal wave (Figure S6; ΔVoltage: 1.26 ± 0.09 mV, n = 5), suggesting that EAAT-mediated glutamate uptake, which is known to be electrogenic (Owe et al., 2006), is performed least in part by MGs.

ON CBCs are depolarized via gap-junctions and cation-nonselective conductances during stage III waves

The experiments described so far define circuit mechanisms that offset the activity of ON and OFF RGCs and thus pattern glutamatergic waves. During these experiments we found that ON CBCs depolarize in each wave and control the activity of downstream neurons. To gain insight into the mechanisms by which glutamatergic waves are initiated and propagated laterally, we focused next on how ON CBCs depolarize.

Dual voltage-clamp recordings showed that ON CBCs receive excitatory inputs in phase with ON RGCs (Figure 6A and 6B; PT: 28 ± 62 ms, n = 8). Surprisingly, for half of the ON CBCs (14/27 cells) the amplitude of wave-associated currents was similar at 0 mV and −60 mV. To better characterize the excitatory conductances of ON CBCs, we blocked inhibition and recorded wave-associated currents at a series of different holding potentials. ON CBCs studied in this way fell into two distinct groups. In the first group (I, 3/6 cells), the current amplitude relative to baseline was insensitive to the holding potential (Figure 6C and 6D). This behavior is expected if the recorded cells are coupled via gap junctions to neighboring neurons that depolarize during stage III waves. In the second group (II, 3/6 cells), wave-associated currents reversed near 0 mV (Figure 6E and 6F), indicative of cation-nonselective conductances. OFF CBCs (4/4) displayed similar current-voltage (I-V) relationships to group II ON CBCs (Figure S4).

Extrasynaptic glutamate directly and indirectly activates ON CBCs

Given previously observed wave-associated increases in extrasynaptic glutamate in the IPL (Blankenship et al., 2009; Firl et al., 2013), the most parsimonious explanation for the cation-nonselective currents is that a subset of developing ON CBCs express ionotropic glutamate receptors (iGluRs) on their axons. To further explore this possibility and elucidate how the two excitatory mechanisms of ON CBCs may be coordinated, we focally applied glutamate onto their axon terminals in retinal slices (P11–13; Figure 7A). These experiments, conducted in absence of Ca^{2+} to block synaptic transmission, recapitulated the ON CBC groupings observed during stage III wave recordings. In 7/11 ON CBCs (group I, Figure 7B), glutamate puffs elicited currents with amplitudes independent of the holding potential and in 4/11 ON CBCs (group II, Figure 7C) glutamate activated currents that reversed near 0 mV. These results indicate that group I ON CBCs are gap-junctionally coupled to neurons that are depolarized by glutamate, whereas group II ON CBCs appear to be directly activated via iGluRs. Importantly, both mechanisms are jointly recruited by extrasynaptic glutamate. Focal glutamate applications on RBC axons elicited currents that reversed at negative potentials (Figure 7D, n = 5) and thus are likely carried by chloride.

Blockade of ionotropic glutamate receptors or gap junctions suppress stage III waves

The observation that group I and II ON CBCs are activated by glutamate, which they release, suggests that both mechanisms may collaborate to propagate and/or initiate stage III waves. To begin to test this hypothesis, we applied blockers of AMPA/kainate (NBQX, 20 μM) and NMDA (AP5, 90 μM) receptors while recording from CBCs and RGCs. In all cases (5/5), NBQX and AP5 reversibly blocked not only EPSCs in RGCs, but also the depolarizations of ON CBCs (Figure 7E and 7F). Waves were similarly eliminated in OFF CBCs and diffuse ACs. Next, we applied meclofenamic acid (MFA, 200 nM), a blocker of gap junctions (Pan et al., 2007; Veruki and Hartveit, 2009), during dual recordings of CBCs and RGCs. Similar to NBQX and AP5, MFA uniformly (6/6) abolished EPSCs in RGCs as well as depolarizations of ON CBCs and diffuse ACs, and the hyperpolarizations of OFF CBCs (Figure 7G and 7H). In agreement with recent data (Veruki and Hartveit, 2009), even with fast solution exchange, the effects of MFA showed slow onset and recovery kinetics (> 20 min). To test whether this accounts for our previous failure to silence stage III waves

with MFA in multielectrode array (MEA) recordings (Kerschensteiner and Wong, 2008), we repeated these experiments. Indeed, when allowing for prolonged exposure and washout, we confirmed that MFA reversibly suppresses stage III waves irrespective of the recording method (Figure S7A and S7B). Moreover, 18-β-Glycyrrhetinic acid (18-β-GA, 50 μM), another blocker of gap junctions, similarly inhibited stage III waves in MEA recordings (Figure S7C and S7D).

Together these data suggest that gap junctions and glutamatergic transmission form interacting circuit mechanisms for lateral excitation of ON CBCs, which are both required for the propagation and/or initiation of stage III waves.

DISCUSSION

In waves of all stages (I - III) bursts of RGC activity spread across the retina separated by periods of silence (Demas et al., 2003; Wong, 1999). Uniquely during stage III (P10 −14), neighboring ON and OFF RGCs are recruited sequentially (ON before OFF) into passing waves (Kerschensteiner and Wong, 2008). This asynchronous activity is thought to help segregate ON and OFF circuits in the dLGN and shape emerging ON and OFF columns in geniculocortical projections (Cramer and Sur, 1997; Dubin et al., 1986; Gjorgjieva et al., 2009; Hahm et al., 1991; Jin et al., 2008; Kerschensteiner and Wong, 2008). At the same time the lateral propagation of stage III waves and the asynchronous firing of RGCs in both eyes appear to maintain retinotopic organization and eye-specific segregation of retinofugal projections (Chapman, 2000; Demas et al., 2006; Zhang et al., 2012).

RGC spiking during stage III waves is known to depend on glutamate release from BCs and a transient rise in extrasynaptic glutamate in the IPL has been shown to accompany each wave (Blankenship et al., 2009; Firl et al., 2013; Wong et al., 2000). But, how stage III waves are initiated and propagated and what mechanisms offset the activity of ON and OFF RGCs was unclear. Using systematic combinations of dual patch clamp recordings we identify intersecting lateral excitatory and vertical inhibitory circuits in the developing retina (Figure 8) and elucidate mechanisms by which neurons in these circuits generate precisely patterned stage III waves.

Circuit mechanisms desynchronizing ON and OFF RGC bursts during stage III waves

Analyzing the mechanisms that generate asynchronous spike bursts, we found that EPSCs in ON and OFF RGCs occur in a stereotypical sequence (ON before OFF), whereas both neurons receive inhibition simultaneously during the ON phase of stage III waves (Figure 1). In addition to distinctions in timing, ON RGCs tend to receive more excitation than inhibition and OFF RGCs more inhibition than excitation. Similar patterns of synaptic inputs to ON and OFF RGCs are elicited by light stimulation in mature retinal circuits (Murphy and Rieke, 2006; Pang et al., 2003) and differences in excitation/inhibition ratios of ON and OFF RGCs persist after photoreceptor degeneration (Margolis et al., 2008; Yee et al., 2012). This suggests that key circuits in the inner retina, particularly those mediating ON-to-OFF crossover inhibition, are established prior to vision, maintained following its loss, and play an important role in patterning both spontaneous and light-evoked RGC activity.

Because inhibition stereotypically precedes excitation to OFF RGCs during stage III waves and light-evoked spike trains of OFF RGCs are shaped by disinhibition (Manookin et al., 2008; Murphy and Rieke, 2006), we tested the contribution of postinhibitory rebound to the delayed bursting of OFF RGCs (Figure S1). Unlike in mature OFF RGCs (Margolis and Detwiler, 2007), we found that rebound depolarizations following somatic current injections rarely elicited spikes at P11–13, and observed no differences in the intrinsic excitability of ON and OFF RGCs (Myhr et al., 2001). With the caveat that somatic current injections may

not adequately capture the influence of dendritic inhibition (Gidon and Segev, 2012), we therefore conclude that offset excitatory synaptic inputs account for the sequential spiking of ON and OFF RGCs.

Asynchronous excitation of RGCs suggested that ON and OFF CBCs, which provide input to ON and OFF RGCs, respectively, participate differently in stage III waves. Indeed, we found that during the ON phase of each wave ON CBCs depolarize, whereas OFF CBCs hyperpolarize (Figure 2). In conjunction with the timing of RGC EPSCs, these data imply that OFF CBCs release glutamate as their voltage returns to baseline following transient hyperpolarizations. The ability of CBCs to continuously vary neurotransmission as a function of voltage relies on the specialized release machinery of ribbon synapses (Matthews and Fuchs, 2010). The importance of ribbon synapses to stage III waves is underlined by the observation that these waves first appear as synaptic ribbons are being assembled in the IPL (Fisher, 1979), a period that is predated by conventional glutamate release from CBCs (Johnson et al., 2003). The mechanisms by which an OFF CBCs return to baseline voltage without appreciable overshoot (Figure 2) is translated into a phasic EPSC in OFF RGCs are discussed in the supplement (Supplemental Discussion).

To maintain the temporal separation of glutamate release from ON and OFF CBCs in the EPSCs of ON and OFF RGCs, the spread of extrasynaptic glutamate during waves needs to be limited to the distinct sublaminae in which their dendrites stratify. Application of TBOA synchronized excitatory input to ON and OFF RGCs (Figure 5), indicating that glutamate uptake via EAATs is necessary to prevent spillover between ON and OFF sublaminae. MGs express EAAT1 (GLAST) and are thought to be the primary agent of glutamate clearance from the IPL (Pow et al., 2000). While Ca^{2+} signals in MGs do not coincide with neuronal waves (Firl et al., 2013), we find that MGs depolarize during each stage III wave (Figure S6), likely reflecting electrogenic glutamate uptake (Owe et al., 2006).

In daylight, OFF CBCs hyperpolarize in part due to decreases in glutamate release from cone photoreceptors onto AMPA and kainate receptors on their dendrites (DeVries, 2000; DeVries and Schwartz, 1999). In contrast, voltage clamp recordings showed that inhibitory synaptic conductances mediate the hyperpolarization of OFF CBCs during stage III waves (Figure 3). In agreement with a previous study (Schubert et al., 2008), we found that both GABA and glycine receptors mediate presynaptic inhibition of developing OFF CBCs. ACs are a diverse class of interneurons in the inner retina (MacNeil and Masland, 1998). The most likely candidates for providing crossover inhibition from ON to OFF CBCs are diffusely stratified Acs, which contact both neurons. To convey directional ON-to-OFF inhibition, diffuse Acs would have to preferentially receive input in the ON sublamina and provide output in the OFF sublamina of the IPL. Consistent with this prediction, we find that diffuse Acs receive excitatory input and depolarize selectively during the ON phase of stage III waves, which in turn matches the timing of inhibitory input to OFF CBCs. This applies to both narrow- and medium field diffuse Acs, which are likely glycinergic and GABAergic, respectively (Masland, 2012; Menger et al., 1998). Finally, blockade of crossover inhibition was sufficient to invert OFF CBC responses and synchronize excitatory inputs to and spiking of ON and OFF RGCs (Figures 3, 5 and S5), supporting the notion that inhibition of OFF CBC axon terminals controls their glutamate release during stage III waves.

A similar “axonal” mode of OFF CBC operation relays signals near the threshold for vision (Murphy and Rieke, 2006) and contributes to processing at higher light levels (Liang and Freed, 2010; Manookin et al., 2008; Molnar and Werblin, 2007). The respective circuits differ in that RBCs rather than ON CBCs drive crossover inhibition at low light levels, but appear not to participate in stage III waves. In addition, light-evoked crossover inhibition can largely be accounted for by activation of glycinergic AII ACs (Liang and Freed, 2010;

Molnar and Werblin, 2007; Murphy and Rieke, 2006), whereas presynaptic inhibition of OFF CBCs during glutamatergic waves involves a broader set of glycinergic (including AII) and GABAergic diffuse ACs.

Circuit mechanisms of stage III wave initiation and propagation

The data discussed so far reveal that ON CBCs engage specific vertical inhibitory circuits to generate precisely timed asynchronous spike bursts in ON and OFF RGCs and thus pattern stage III waves. Next, we will address how excitation spreads laterally between ON CBCs to provide insight into the mechanisms that initiate and propagate stage III waves.

Voltage-clamp recordings showed that ON CBCs fall into two groups that receive excitatory input via distinct mechanisms. In one group (II), stage III waves as well as focal glutamate applications on axon terminals appear to activate cation-nonselective conductances (Figures 6 and 7). In vision, ON CBCs hyperpolarize to glutamate release from cones via dendritically localized mGluRs coupled to Trpm1 channels (Koike et al., 2010; Masu et al., 1995; Morgans et al., 2009). Based on our results, the most parsimonious conclusion is that during development group II ON CBCs express iGluRs on their axon terminals. While expression of these receptors is likely transient, there is some evidence that even in mature circuits a subset of ON CBCs may utilize iGluRs (Kamphuis et al., 2003; Pang et al., 2012). Wave-associated spillover of glutamate into the extrasynaptic space (Blankenship et al., 2009; Firl et al., 2013) combined with the expression of axonal iGluRs would provide a direct excitatory link between neighboring ON CBCs.

In another group (I) of ON CBCs, gap junctions mediate depolarizations during waves and in response to focal glutamate applications (Figure 7). Which neurons form these gap junctions with ON CBCs? Candidates have to depolarize during the ON phase of stage III waves and be activated by glutamate. In mature circuits, ON CBCs are known to couple to AII ACs, which express iGluRs (Hartveit and Veruki, 1997; Kolb and Famiglietti, 1974; Mills and Massey, 1995; Veruki and Hartveit, 2002; Zhou and Dacheux, 2004). In addition to participating in visual processing, these electrical connections are involved in the generation of patterned spontaneous activity in retinas with photoreceptor degeneration (Borowska et al., 2011; Trenholm et al., 2012). Among the diffuse ACs we recorded, four were morphologically identified as AII ACs. Each depolarized during the ON phase of stage III waves. Aside from excitatory coupling to ON CBCs, AII ACs likely participate in glycinergic crossover inhibition of OFF CBCs and OFF RGCs. In addition to AII ACs, ON CBCs may be coupled to other ACs (Farrow et al., 2013) and/or each other (Arai et al., 2010). Thus, gap junctions provide a second lateral excitatory link, either direct or via intermediate ACs, among ON CBCs.

Both forms of excitatory input are recruited by glutamate released from ON CBCs, which we propose forms the basis for the generation and coordinated lateral propagation of stage III waves. Consistent with this notion, blockade of either iGluRs or gap junctions was sufficient to block stage III waves in ON CBCs as well as RGCs (Figures 7 and S7). In support of the importance of gap junctions, we show that application of MFA blocks depolarizations in ON CBCs, and that both MFA and 18-β-GA reversibly silence stage III waves in MEA recordings. In previous studies, 18-β-GA similarly suppressed glutamatergic waves in the developing chick and rabbit retina (Syed et al., 2004; Wong et al., 1998). However, stage III waves persist in knockout mice lacking two connexin subunits involved in coupling of BCs (Blankenship et al., 2011). One or both of the following explanations likely account for the discrepant results of pharmacologic and genetic manipulations. First, blockers of gap junctions are known to have off target effects (Peretz et al., 2005). While MFA and 18-β-GA are among the more specific antagonists of gap junctions (Pan et al., 2007) and the similarity of their effects in our experiments argue against a non-specific

mechanism of wave blockade, we cannot rule out this possibility. Second, genetic (i.e. persistent) manipulations that interfere with specific wave mechanisms have consistently been found to trigger homeostatic adjustments that preserve waves (Blankenship et al., 2009; Stacy et al., 2005; Stafford et al., 2009; Sun et al., 2008). Accordingly, germline deletion of connexins may lead to compensatory changes in iGluR expression of ON CBCs. While future experiments are needed to conclusively determine the importance of gap junctions for the propagation and/or initiation of stage III waves, our recordings demonstrate that they are responsible for the depolarization of group I ON CBCs.

Spontaneous network activity in the retina and elsewhere arises either from pacemaker neurons or in a distributed manner from groups of neurons coupled by excitatory mechanisms (Blankenship and Feller, 2010). Blockade of either gap junctions or iGluRs suppressed all depolarizations in ON CBCs (Figure 7). While our sampling of ON CBCs is not exhaustive and other neurons (e.g. AII ACs) could act as pacemakers (Trenholm et al., 2012), these data favor a distributed origin of stage III waves and argue that the two excitatory links between ON CBCs we discover are involved both in the initiation and lateral propagation of network activity.

EXPERIMENTAL PROCEDURES

Electrophysiology

All procedures in this study were approved by the Animal Studies Committee of Washington University School of Medicine and performed in compliance with the National Institutes of Health *Guide for the Care and Use of Laboratory Animals*. Mice (C57BL/6J) were dark adapted (~2 hrs) and their retinas isolated under infrared illumination (> 900 nm) as described previously (Soto et al., 2012).

Dual whole-cell patch clamp recordings from RGCs and cells in the inner nuclear layer (INL) were obtained in flat mount preparations continuously superfused (~2 mL/min) with warm (33–35 °C) mouse artificial cerebrospinal (mACSF) containing (in mM) 125 NaCl, 2.5 KCl, 1 $MgCl_2$, 1.25 NaH_2PO_4, 2 $CaCl_2$, 20 glucose and 26 $NaHCO_3$ equilibrated with 95% O_2 / 5% CO_2. In some experiments, the following pharmacological agents were added to mACSF and bath-applied individually or in combinations (s. Results): D-(-)-2-Amino-5-phosphonopentanoic acid (AP5, 90 μM, Tocris), 2,3-Dioxo-6-nitro-1,2,3,4-tetrahydrobenzo[*f*]quinoxaline-7-sulfonamide (NBQX, 20 μM, Tocris), (1,2,5,6-Tetrahydropyridine-4-yl-methylphosphinic acid (TPMPA, 50 nM, Sigma), gabazine (5 μM, Tocris), Strychnine (500 nM, Sigma), Meclofenamic acid (MFA, 200 μM, Sigma) and 18-β-Glycyrrhetinic acid (18-β-GA, 50 μM, Sigma). To record from monostratified RGCs with overlapping dendrites, neighboring large somata (~20 μm) in the ganglion cell layer (GCL) were targeted after tearing a hole through the inner limiting membrane (ILM). To record INL cells within the dendritic territory of a given RGC, an additional hole in the ILM was made ~100 μm from the site of the RGC recording and patch electrodes advanced diagonally towards the INL. Cells were targeted for recording under infrared (> 900 nm) illumination.

Responses of BCs to focal glutamate applications on their axon terminals were recorded in retinal slices (200 μm thick). For slicing, pieces of isolated retinas were embedded in low melting point agarose (3 %, Sigma) and cut on a vibrating microtome (Leica). In the recording chamber slices were held in place by a harp consisting of nylon strings glued to a platinum ring. Glutamate (1 mM in mACSF, Sigma) was focally applied in short (30 ms) puffs from a patch pipette using a Picospritzer II (Parker Hannifin). We included 0.1 mM Alexa488 in the puff solution and verified by 2-photon imaging that applications were restricted to axon terminals of BCs filled with Alexa568.

For voltage clamp recordings from RGCs, patch pipettes (4 – 7 MΩ, borosilicate glass) were filled with (in mM) 120 Cs-gluconate, 1 $CaCl_2$, 1 $MgCl_2$, 10 Na-HEPES, 11 EGTA, 10 TEA-Cl and 2 Qx314 (pH adjusted to 7.2 with CsOH). For all current clamp recordings and voltage clamp recordings from INL cells, patch pipettes were filled with (in mM) 125 K-gluconate, 10 NaCl, 1 $MgCl_2$, 10 EGTA, 5 HEPES, 5 ATP-Na and 0.1 GTP-Na (pH adjusted to 7.2 with KOH). For glutamate puff experiments K-gluconate in the pipette solution was replaced by Cs-gluconate and pH adjusted with CsOH. Internal solutions included 0.1 mM of either Alexa 488 or Alexa 568. All reported voltages were corrected for liquid junction potentials. Signals were amplified on Multiclamp 700B amplifier, filtered at 3 kHz (8-pole Bessel low-pass) and sampled at 10 kHz. All recordings of spontaneous activity were conducted in darkness (< 0.1 Rh*/R/s).

In MEA experiments, action potentials from large ensembles of RGCs were simultaneously recorded on planar arrays of 252 electrodes (MultiChannelSystems). Towards this end, rectangular pieces of isolated retina were mounted on the MEAs RGC-side down and secured with a dialysis membrane weighed down by a platinum ring. The tissue was superfused (~1 mL/min) with warm (33–35 °C) mouse artificial cerebrospinal (mACSF). Signals of each electrode were bandpass filtered between 0.3 and 3 kHz and digitized at 5 kHz. Signal cutouts flanking (3 ms) negative threshold crossings were recorded to hard disk and principal component analysis of these waveforms used to sort spikes into trains representing the activity of individual neurons (Offline Sorter; Plexon). Refractory periods in spike trains were used to assess the quality of the sorting. Crosscorrelations among spike trains were used to detect when activity of a single neuron had been recorded on more than one electrode. In these cases, only the train with the most spikes was used for further analysis.

Imaging

The morphology of recorded cells (filled with Alexa488 and Alexa568) was analyzed in 2-photon z-series image stacks acquired at the end of each recording (Microscope: Fv1000 MPE; Objective: 20x, 0.9NA, both Olympus). Neurons were identified as ON or OFF cells when their dendrites (RGCs), axons (BCs) or bifunctional neurites (ACs) stratified within the inner 3/5 and outer 2/5, respectively, of the inner plexiform layer (IPL) (Ghosh et al., 2004). ACs that elaborate neurites in both parts of the IPL were classified as diffuse ACs. In a subset of our experiments full-field light stimuli (~10,000 Rh*/R/s) were presented on an organic light-emitting display (852×600 pixels, OLED-XL, eMagin) focused onto the photoreceptors via the substage condenser. In each case, the elicited responses confirmed the morphology-based assignment of the respective neurons to ON or OFF groups. In the INL, we recorded BCs, ACs and MGs, which were distinguished based on their morphology (Supplemental Experimental Procedures).

Analysis

Data were analyzed using procedures custom written in Matlab (Mathworks). To compare the timing of synaptic inputs to and activity of simultaneously recorded cells we computed crosscorrelations, as follows:

$$C_{xy}(t)=\begin{cases}\dfrac{\frac{1}{N-t/\Delta t}\times\sum_{i=1}^{N-t/\Delta t}(x_i-\langle x\rangle)\times\left(y_{i+t/\Delta t}-\langle y\rangle\right)}{\sqrt{\frac{1}{N}\sum_{i=1}^{N}(x_i-\langle x\rangle)^2}\times\sqrt{\frac{1}{N}\sum_{i=1}^{N}(y_i-\langle y\rangle)^2}} & t\geq 0\\ C_{yx}(-t) & t<0\end{cases}$$

where x_i and y_i represent spike counts, or voltage or conductance measurements of two cells in the i-th of N time bins, <x> and <y> signify their respective average values, and t the time-lag in the crosscorrelation. The width of time bins (Δt) was 100 ms for spike trains and 1 ms for voltage and conductance measurements. Because synaptic inputs and activity were nonstationary (i.e. high during waves and negligible in between), we determined values of <x> and <y> using 5 s-wide sliding windows (Kerschensteiner and Wong, 2008; Perkel et al., 1967).

To algorithmically detect waves in current or voltage recordings of BCs and RGCs, we smoothed the respective traces using a Loess filter and defined excursions of the smoothed traces beyond several standard deviations as periods of waves, which were than analyzed in the original traces. This procedure reliably identified >90 % of the events identified by a human observer. To gauge the significance of coincident activity in simultaneously recorded cells, events of one cell were randomly displaced within the recording.

The overlap of RGC dendrites was quantified as:

$$overlap = \frac{2*(A \cap B)}{A+B}$$

where A and B represent the smallest convex polygons encompassing the arbors of the respective RGCs in a z-projection and $A \cap B$ indicates the area of their intersection.

We used either Wilcoxon-Mann-Whitney rank sum or, in case of paired samples, Wilcoxon signed-rank tests to assess statistical significance of differences between groups. Throughout the text population averages are given as mean ± standard error of the mean (SEM).

Supplementary Material

Refer to Web version on PubMed Central for supplementary material.

Acknowledgments

We thank members of the Kerschensteiner Lab and Dr. Peter Lukasiewicz for helpful discussions and comments on the manuscript. We are grateful to Dr. Peter Lukasiewicz for lending us equipment for focal agonist applications and to Dr. Felice Dunn for advice on bipolar cell recordings in retinal flat mount preparations. This work was supported by grants from the Whitehall Foundation (DK), Edward Mallinckrodt Jr. Foundation (DK), Alfred P. Sloan Foundation (DK), Research to Prevent Blindness Foundation (Career Development Award to DK and unrestricted grant to the Dept. of Ophthalmology and Visual Sciences at Washington University), the NIH (R01 EY021855 to DK; P30 EY0268 to the Dept. of Ophthalmology and Visual Sciences at Washington University) and the NSF (DGE1143954, AA).

REFERENCES

Ackman JB, Burbridge TJ, Crair MC. Retinal waves coordinate patterned activity throughout the developing visual system. Nature. 2012; 490:219–225. [PubMed: 23060192]

Arai I, Tanaka M, Tachibana M. Active roles of electrically coupled bipolar cell network in the adult retina. J Neurosci. 2010; 30:9260–9270. [PubMed: 20610761]

Blankenship AG, Feller MB. Mechanisms underlying spontaneous patterned activity in developing neural circuits. Nat Rev Neurosci. 2010; 11:18–29. [PubMed: 19953103]

Blankenship AG, Ford KJ, Johnson J, Seal RP, Edwards RH, Copenhagen DR, Feller MB. Synaptic and extrasynaptic factors governing glutamatergic retinal waves. Neuron. 2009; 62:230–241. [PubMed: 19409268]

Blankenship AG, Hamby AM, Firl A, Vyas S, Maxeiner S, Willecke K, Feller MB. The role of neuronal connexins 36 and 45 in shaping spontaneous firing patterns in the developing retina. J Neurosci. 2011; 31:9998–10008. [PubMed: 21734291]

Borowska J, Trenholm S, Awatramani GB. An intrinsic neural oscillator in the degenerating mouse retina. J Neurosci. 2011; 31:5000–5012. [PubMed: 21451038]

Butts DA, Kanold PO, Shatz CJ. A burst-based "Hebbian" learning rule at retinogeniculate synapses links retinal waves to activity-dependent refinement. PLoS Biol. 2007; 5:e61. [PubMed: 17341130]

Chandrasekaran AR, Shah RD, Crair MC. Developmental homeostasis of mouse retinocollicular synapses. J Neurosci. 2007; 27:1746–1755. [PubMed: 17301182]

Chapman B. Necessity for afferent activity to maintain eye-specific segregation in ferret lateral geniculate nucleus. Science. 2000; 287:2479–2482. [PubMed: 10741966]

Cramer KS, Sur M. Blockade of afferent impulse activity disrupts on/off sublamination in the ferret lateral geniculate nucleus. Brain Res Dev Brain Res. 1997; 98:287–290.

Demas J, Eglen SJ, Wong RO. Developmental loss of synchronous spontaneous activity in the mouse retina is independent of visual experience. J Neurosci. 2003; 23:2851–2860. [PubMed: 12684472]

Demas J, Sagdullaev BT, Green E, Jaubert-Miazza L, McCall MA, Gregg RG, Wong RO, Guido W. Failure to maintain eye-specific segregation in nob, a mutant with abnormally patterned retinal activity. Neuron. 2006; 50:247–259. [PubMed: 16630836]

DeVries SH. Bipolar cells use kainate and AMPA receptors to filter visual information into separate channels. Neuron. 2000; 28:847–856. [PubMed: 11163271]

DeVries SH, Schwartz EA. Kainate receptors mediate synaptic transmission between cones and 'Off' bipolar cells in a mammalian retina. Nature. 1999; 397:157–160. [PubMed: 9923677]

Dubin MW, Stark LA, Archer SM. A role for action-potential activity in the development of neuronal connections in the kitten retinogeniculate pathway. J Neurosci. 1986; 6:1021–1036. [PubMed: 3701407]

Farrow K, Teixeira M, Szikra T, Viney TJ, Balint K, Yonehara K, Roska B. Ambient illumination toggles a neuronal circuit switch in the retina and visual perception at cone threshold. Neuron. 2013; 78:325–338. [PubMed: 23541902]

Firl A, Sack GS, Newman ZL, Tani H, Feller MB. Extrasynaptic glutamate and inhibitory neurotransmission modulate ganglion cell participation during glutamatergic retinal waves. J Neurophysiol. 2013; 109:1969–1978. [PubMed: 23343894]

Fisher LJ. Development of synaptic arrays in the inner plexiform layer of neonatal mouse retina. J Comp Neurol. 1979; 187:359–372. [PubMed: 489784]

Ghosh KK, Bujan S, Haverkamp S, Feigenspan A, Wassle H. Types of bipolar cells in the mouse retina. J Comp Neurol. 2004; 469:70–82. [PubMed: 14689473]

Gidon A, Segev I. Principles governing the operation of synaptic inhibition in dendrites. Neuron. 2012; 75:330–341. [PubMed: 22841317]

Gjorgjieva J, Toyoizumi T, Eglen SJ. Burst-time-dependent plasticity robustly guides ON/OFF segregation in the lateral geniculate nucleus. PLoS Comput Biol. 2009; 5:e1000618. [PubMed: 20041207]

Grubb MS, Rossi FM, Changeux JP, Thompson ID. Abnormal functional organization in the dorsal lateral geniculate nucleus of mice lacking the beta 2 subunit of the nicotinic acetylcholine receptor. Neuron. 2003; 40:1161–1172. [PubMed: 14687550]

Hahm JO, Langdon RB, Sur M. Disruption of retinogeniculate afferent segregation by antagonists to NMDA receptors. Nature. 1991; 351:568–570. [PubMed: 1675433]

Hartveit E, Veruki ML. AII amacrine cells express functional NMDA receptors. Neuroreport. 1997; 8:1219–1223. [PubMed: 9175117]

Jin JZ, Weng C, Yeh CI, Gordon JA, Ruthazer ES, Stryker MP, Swadlow HA, Alonso JM. On and off domains of geniculate afferents in cat primary visual cortex. Nat Neurosci. 2008; 11:88–94. [PubMed: 18084287]

Johnson J, Tian N, Caywood MS, Reimer RJ, Edwards RH, Copenhagen DR. Vesicular neurotransmitter transporter expression in developing postnatal rodent retina: GABA and glycine precede glutamate. J Neurosci. 2003; 23:518–529. [PubMed: 12533612]

Kamphuis W, Klooster J, Dijk F. Expression of AMPA-type glutamate receptor subunit (GluR2) in ON-bipolar neurons in the rat retina. J Comp Neurol. 2003; 455:172–186. [PubMed: 12454983]

Katz LC, Shatz CJ. Synaptic activity and the construction of cortical circuits. Science. 1996; 274:1133–1138. [PubMed: 8895456]

Kerschensteiner D, Wong RO. A precisely timed asynchronous pattern of ON and OFF retinal ganglion cell activity during propagation of retinal waves. Neuron. 2008; 58:851–858. [PubMed: 18579076]

Koike C, Obara T, Uriu Y, Numata T, Sanuki R, Miyata K, Koyasu T, Ueno S, Funabiki K, Tani A, et al. TRPM1 is a component of the retinal ON bipolar cell transduction channel in the mGluR6 cascade. Proc Natl Acad Sci U S A. 2010; 107:332–337. [PubMed: 19966281]

Kolb H, Famiglietti EV. Rod and cone pathways in the inner plexiform layer of cat retina. Science. 1974; 186:47–49. [PubMed: 4417736]

Lee CW, Eglen SJ, Wong RO. Segregation of ON and OFF retinogeniculate connectivity directed by patterned spontaneous activity. J Neurophysiol. 2002; 88:2311–2321. [PubMed: 12424272]

Liang Z, Freed MA. The ON pathway rectifies the OFF pathway of the mammalian retina. J Neurosci. 2010; 30:5533–5543. [PubMed: 20410107]

Liets LC, Olshausen BA, Wang GY, Chalupa LM. Spontaneous activity of morphologically identified ganglion cells in the developing ferret retina. J Neurosci. 2003; 23:7343–7350. [PubMed: 12917368]

MacNeil MA, Masland RH. Extreme diversity among amacrine cells: implications for function. Neuron. 1998; 20:971–982. [PubMed: 9620701]

Manookin MB, Beaudoin DL, Ernst ZR, Flagel LJ, Demb JB. Disinhibition combines with excitation to extend the operating range of the OFF visual pathway in daylight. J Neurosci. 2008; 28:4136–4150. [PubMed: 18417693]

Margolis DJ, Detwiler PB. Different mechanisms generate maintained activity in ON and OFF retinal ganglion cells. J Neurosci. 2007; 27:5994–6005. [PubMed: 17537971]

Margolis DJ, Newkirk G, Euler T, Detwiler PB. Functional stability of retinal ganglion cells after degeneration-induced changes in synaptic input. J Neurosci. 2008; 28:6526–6536. [PubMed: 18562624]

Masland RH. The tasks of amacrine cells. Vis Neurosci. 2012; 29:3–9. [PubMed: 22416289]

Masu M, Iwakabe H, Tagawa Y, Miyoshi T, Yamashita M, Fukuda Y, Sasaki H, Hiroi K, Nakamura Y, Shigemoto R, et al. Specific deficit of the ON response in visual transmission by targeted disruption of the mGluR6 gene. Cell. 1995; 80:757–765. [PubMed: 7889569]

Matthews G, Fuchs P. The diverse roles of ribbon synapses in sensory neurotransmission. Nat Rev Neurosci. 2010; 11:812–822. [PubMed: 21045860]

Meister M, Wong RO, Baylor DA, Shatz CJ. Synchronous bursts of action potentials in ganglion cells of the developing mammalian retina. Science. 1991; 252:939–943. [PubMed: 2035024]

Menger N, Pow DV, Wassle H. Glycinergic amacrine cells of the rat retina. J Comp Neurol. 1998; 401:34–46. [PubMed: 9802699]

Miller KD. A model for the development of simple cell receptive fields and the ordered arrangement of orientation columns through activity-dependent competition between ON- and OFF-center inputs. J Neurosci. 1994; 14:409–441. [PubMed: 8283248]

Mills SL, Massey SC. Differential properties of two gap junctional pathways made by AII amacrine cells. Nature. 1995; 377:734–737. [PubMed: 7477263]

Molnar A, Werblin F. Inhibitory feedback shapes bipolar cell responses in the rabbit retina. J Neurophysiol. 2007; 98:3423–3435. [PubMed: 17928553]

Mooney R, Penn AA, Gallego R, Shatz CJ. Thalamic relay of spontaneous retinal activity prior to vision. Neuron. 1996; 17:863–874. [PubMed: 8938119]

Morgan J, Thompson ID. The segregation of ON- and OFF-center responses in the lateral geniculate nucleus of normal and monocularly enucleated ferrets. Vis Neurosci. 1993; 10:303–311. [PubMed: 8485093]

Morgans CW, Zhang J, Jeffrey BG, Nelson SM, Burke NS, Duvoisin RM, Brown RL. TRPM1 is required for the depolarizing light response in retinal ON-bipolar cells. Proc Natl Acad Sci U S A. 2009; 106:19174–19178. [PubMed: 19861548]

Murphy GJ, Rieke F. Network variability limits stimulus-evoked spike timing precision in retinal ganglion cells. Neuron. 2006; 52:511–524. [PubMed: 17088216]

Myhr KL, Lukasiewicz PD, Wong RO. Mechanisms underlying developmental changes in the firing patterns of ON and OFF retinal ganglion cells during refinement of their central projections. J Neurosci. 2001; 21:8664–8671. [PubMed: 11606654]

Owe SG, Marcaggi P, Attwell D. The ionic stoichiometry of the GLAST glutamate transporter in salamander retinal glia. J Physiol. 2006; 577:591–599. [PubMed: 17008380]

Pan F, Mills SL, Massey SC. Screening of gap junction antagonists on dye coupling in the rabbit retina. Vis Neurosci. 2007; 24:609–618. [PubMed: 17711600]

Pang JJ, Gao F, Wu SM. Light-evoked excitatory and inhibitory synaptic inputs to ON and OFF alpha ganglion cells in the mouse retina. J Neurosci. 2003; 23:6063–6073. [PubMed: 12853425]

Pang JJ, Gao F, Wu SM. Ionotropic glutamate receptors mediate OFF responses in light-adapted ON bipolar cells. Vision Res. 2012; 68:48–58. [PubMed: 22842089]

Peretz A, Degani N, Nachman R, Uziyel Y, Gibor G, Shabat D, Attali B. Meclofenamic acid and diclofenac, novel templates of KCNQ2/Q3 potassium channel openers, depress cortical neuron activity and exhibit anticonvulsant properties. Molecular pharmacology. 2005; 67:1053–1066. [PubMed: 15598972]

Perkel DH, Gerstein GL, Moore GP. Neuronal spike trains and stochastic point processes. II. Simultaneous spike trains. Biophys J. 1967; 7:419–440. [PubMed: 4292792]

Pow DV, Barnett NL, Penfold P. Are neuronal transporters relevant in retinal glutamate homeostasis? Neurochemistry international. 2000; 37:191–198. [PubMed: 10812204]

Schubert T, Kerschensteiner D, Eggers ED, Misgeld T, Kerschensteiner M, Lichtman JW, Lukasiewicz PD, Wong RO. Development of presynaptic inhibition onto retinal bipolar cell axon terminals is subclass-specific. J Neurophysiol. 2008; 100:304–316. [PubMed: 18436633]

Shah RD, Crair MC. Retinocollicular synapse maturation and plasticity are regulated by correlated retinal waves. J Neurosci. 2008; 28:292–303. [PubMed: 18171946]

Soto F, Ma X, Cecil JL, Vo BQ, Culican SM, Kerschensteiner D. Spontaneous activity promotes synapse formation in a cell-type-dependent manner in the developing retina. J Neurosci. 2012; 32:5426–5439. [PubMed: 22514306]

Stacy RC, Demas J, Burgess RW, Sanes JR, Wong RO. Disruption and recovery of patterned retinal activity in the absence of acetylcholine. J Neurosci. 2005; 25:9347–9357. [PubMed: 16221843]

Stafford BK, Sher A, Litke AM, Feldheim DA. Spatial-temporal patterns of retinal waves underlying activity-dependent refinement of retinofugal projections. Neuron. 2009; 64:200–212. [PubMed: 19874788]

Sun C, Warland DK, Ballesteros JM, van der List D, Chalupa LM. Retinal waves in mice lacking the beta2 subunit of the nicotinic acetylcholine receptor. Proc Natl Acad Sci U S A. 2008; 105:13638–13643. [PubMed: 18757739]

Syed MM, Lee S, Zheng J, Zhou ZJ. Stage-dependent dynamics and modulation of spontaneous waves in the developing rabbit retina. J Physiol. 2004; 560:533–549. [PubMed: 15308679]

Trenholm S, Borowska J, Zhang J, Hoggarth A, Johnson K, Barnes S, Lewis TJ, Awatramani GB. Intrinsic oscillatory activity arising within the electrically coupled AII amacrine-ON cone bipolar cell network is driven by voltage-gated Na+ channels. J Physiol. 2012; 590:2501–2517. [PubMed: 22393249]

Veruki ML, Hartveit E. Electrical synapses mediate signal transmission in the rod pathway of the mammalian retina. J Neurosci. 2002; 22:10558–10566. [PubMed: 12486148]

Veruki ML, Hartveit E. Meclofenamic acid blocks electrical synapses of retinal AII amacrine and on-cone bipolar cells. J Neurophysiol. 2009; 101:2339–2347. [PubMed: 19279153]

Wong RO. Retinal waves and visual system development. Annu Rev Neurosci. 1999; 22:29–47. [PubMed: 10202531]

Wong RO, Oakley DM. Changing patterns of spontaneous bursting activity of on and off retinal ganglion cells during development. Neuron. 1996; 16:1087–1095. [PubMed: 8663985]

Wong WT, Myhr KL, Miller ED, Wong RO. Developmental changes in the neurotransmitter regulation of correlated spontaneous retinal activity. J Neurosci. 2000; 20:351–360. [PubMed: 10627612]

Wong WT, Sanes JR, Wong RO. Developmentally regulated spontaneous activity in the embryonic chick retina. J Neurosci. 1998; 18:8839–8852. [PubMed: 9786990]

Yee CW, Toychiev AH, Sagdullaev BT. Network deficiency exacerbates impairment in a mouse model of retinal degeneration. Front Syst Neurosci. 2012; 6:8. [PubMed: 22383900]

Zhang J, Ackman JB, Xu HP, Crair MC. Visual map development depends on the temporal pattern of binocular activity in mice. Nat Neurosci. 2012; 15:298–307. [PubMed: 22179110]

Zhang LL, Pathak HR, Coulter DA, Freed MA, Vardi N. Shift of intracellular chloride concentration in ganglion and amacrine cells of developing mouse retina. J Neurophysiol. 2006; 95:2404–2416. [PubMed: 16371454]

Zhou C, Dacheux RF. All amacrine cells in the rabbit retina possess AMPA-, NMDA-, GABA-, and glycine-activated currents. Vis Neurosci. 2004; 21:181–188. [PubMed: 15259569]

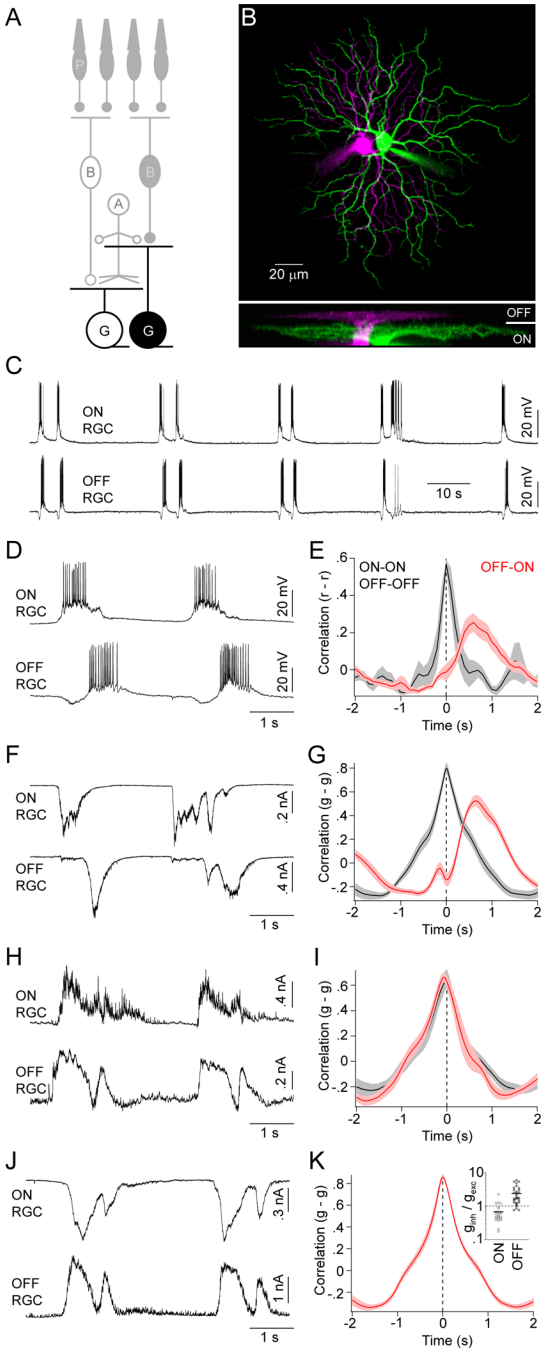

Figure 1. Spike and synaptic input patterns of ON and OFF RGCs during stage III waves

(A) Schematic illustration of the retinal circuitry. Letters denote the following cell classes: P -photoreceptors, B - CBCs, A - ACs, G - RGCs. Light responses are indicated by filled (OFF) or open (ON) somata. Cells recorded to obtain the data of this figure are highlighted. (B) Orthogonal projections of a 2-photon image stack of representative ON (green) and OFF (magenta) RGCs recorded in a flat-mounted P12 retina. (C, D) Representative current-clamp (I = 0 pA) traces of neighboring ON and OFF RGCs shown on different timescales. (E) Crosscorrelations of the firing rates (r) of same (black) and opposite (red) sign RGCs during stage III waves. Lines (shaded areas) here and elsewhere represent the means (± SEMs) of the respective populations (n = 4 for same sign and n = 11 for opposite sign RGCs). (F)

Representative EPSCs (V_M ~ −60 mV) of neighboring ON and OFF RGCs during glutamatergic waves. (G) Crosscorrelations of excitatory conductances (g) of same (n = 10) and opposite sign (n = 10) RGCs. (H) Representative IPSCs (V_M ~ 0 mV) of neighboring ON and OFF RGCs. (I) Crosscorrelations of inhibitory conductances (g) of same (n = 7) and opposite (n = 7) sign RGCs color-coded as in (E) and (G). (I) Simultaneously recorded EPSCs and IPSCs from a representative ON and OFF RGCs. (K) Crosscorrelation (n = 8) of excitatory conductances of ON RGCs and inhibitory conductances of OFF RGCs. The ratios of inhibitory (g_{inh}) and excitatory (g_{exc}) conductances of ON (open circles) and OFF (filled circles) RGCs during stage III waves are shown in an *inset*. Lines indicate the means of the respective populations. See also Figure S1.

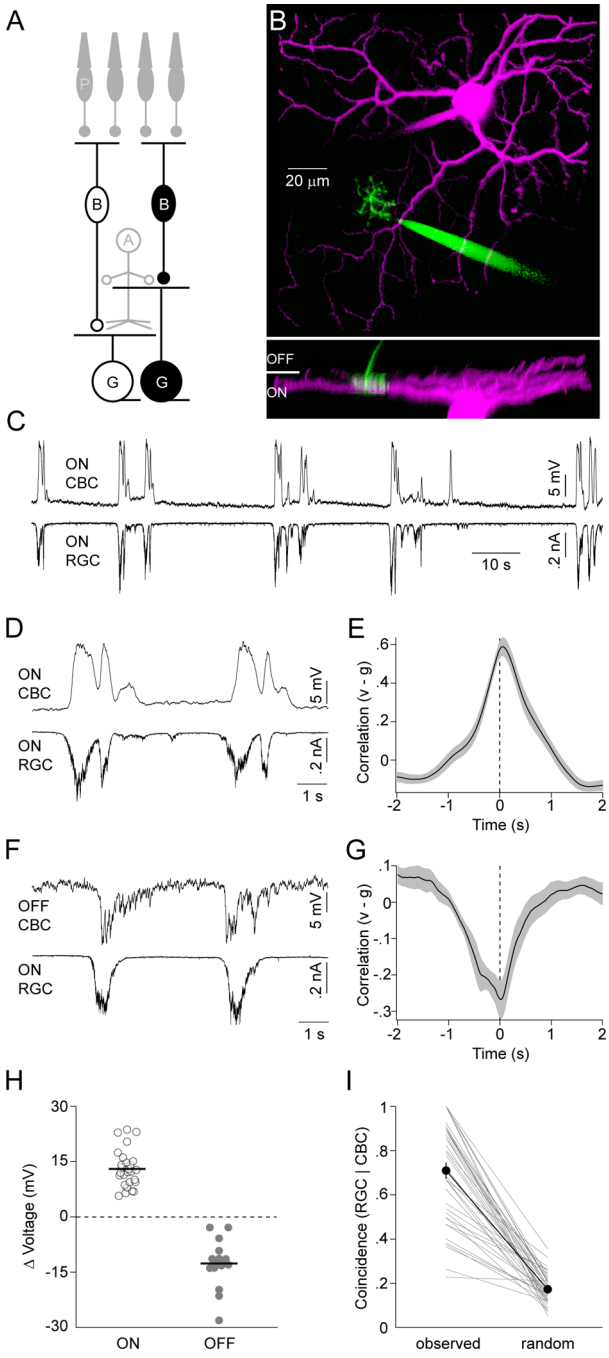

Figure 2. ON CBCs depolarize and OFF CBCs hyperpolarize during stage III waves

(A) Schematic of the retinal circuitry with the cells recorded to obtain data presented in this figure highlighted. Labeling as in Figure 1. (B) Representative 2-photon image stack projected along two orthogonal axes. For visual clarity, the recording electrodes have been digitally removed from the side view (*bottom panel*). (C, D) Simultaneous voltage (I = 0 pA, V_{Rest} ~ −63 mV) and EPSC (V_M ~ −60 mV) recording of an ON CBC and ON RGC, respectively, during stage III waves, shown on different timescales. (E) Crosscorrelation (mean ± SEM, n = 18) of ON CBC voltage (v) and excitatory synaptic conductance of ON RGCs (or inhibitory conductance of OFF RGC) (g). (F) Simultaneous voltage and EPSC recording of an OFF CBC (V_{Rest} ~ −46 mV) and ON RGC. (G) Crosscorrelation (n = 10) of

OFF CBC voltage (v) and excitatory conductance of ON RGCs (or inhibitory conductance of OFF RGC) (g). (H) The average of the maximal voltage changes during each wave of a given CBC is indicated by circles (open - ON, filled - OFF). Population averages are shown by lines. (I) The conditional probability of algorithmically detecting a wave in an ON RGC EPSC trace given that a wave was identified in the simultaneously recorded CBC voltage is depicted. Thin lines indicate data from each dual recording. The thick line and filled symbols (errorbars) represent the mean (± SEM) of the population. See also Figure S2.

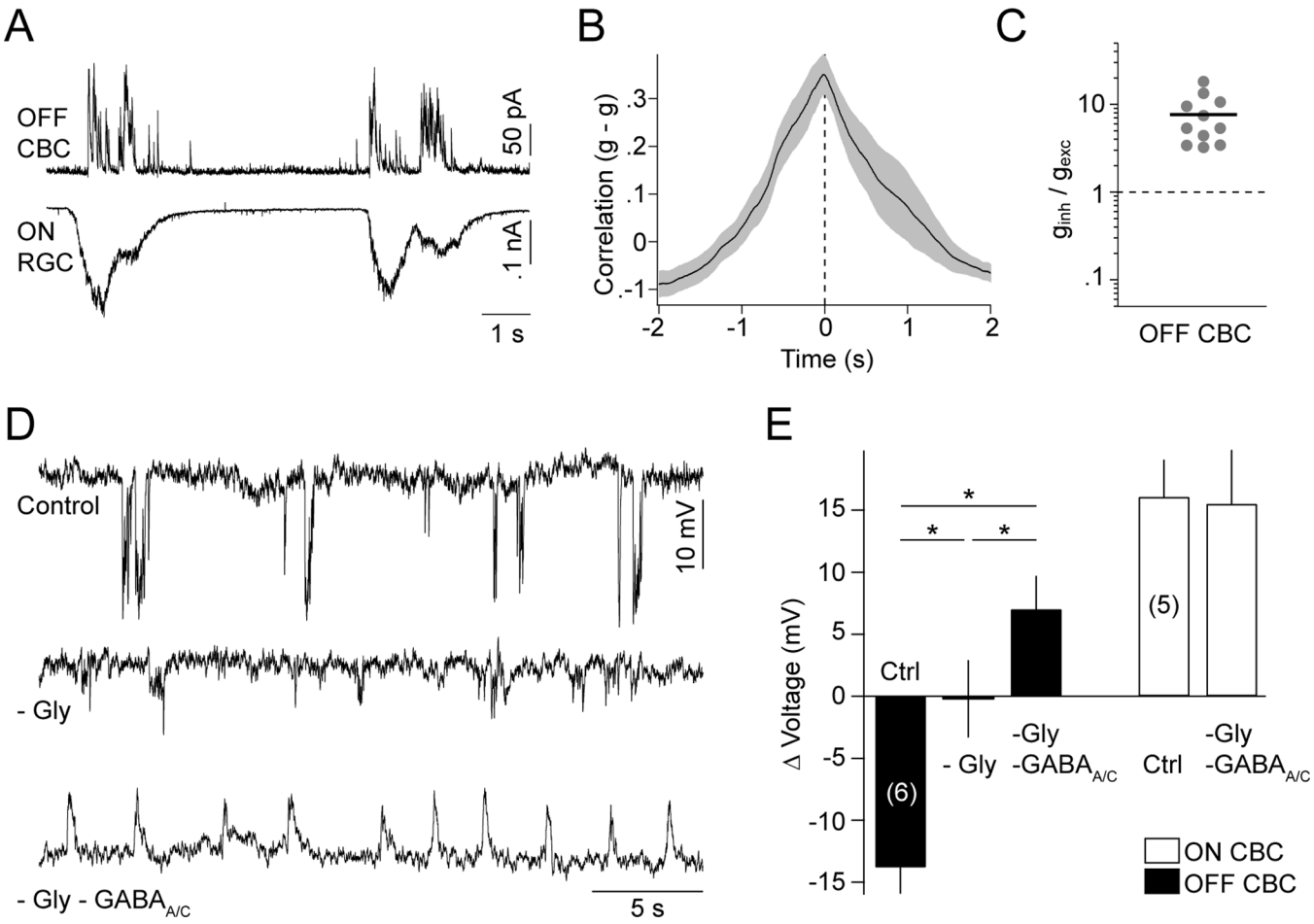

Figure 3. Glycinergic and GABAergic crossover inhibition hyperpolarizes OFF CBCs during each wave

(A) Simultaneous recording of wave-associated IPSCs (V_M ~ 0 mV) in OFF CBCs and EPSCs (V_M ~ −60 mV) in ON RGCs. (B) Crosscorrelation (mean ± SEM, n = 7) of inhibitory synaptic conductances of OFF CBCs and excitatory synaptic conductances of ON RGCs. (C) Ratio of inhibitory (g_{inh}) and excitatory (g_{exc}) synaptic conductances activated in OFF CBCs (filled circles) during stage III waves. Line indicates mean of the population. (D) Voltage traces of OFF CBCs in control conditions *(top trace)*, in the presence of strychnine (500 nM, *middle trace)*, and strychnine (500 nM), gabazine (5 μM) and TPMPA (50 μM) *(bottom trace)*. (E) Group data (mean ± SEM) for ON (white bars) and OFF (black bars) CBCs illustrating the cell-type-specific effects of inhibitory blockers on stage III voltage responses. See also Figures S3 and S4.

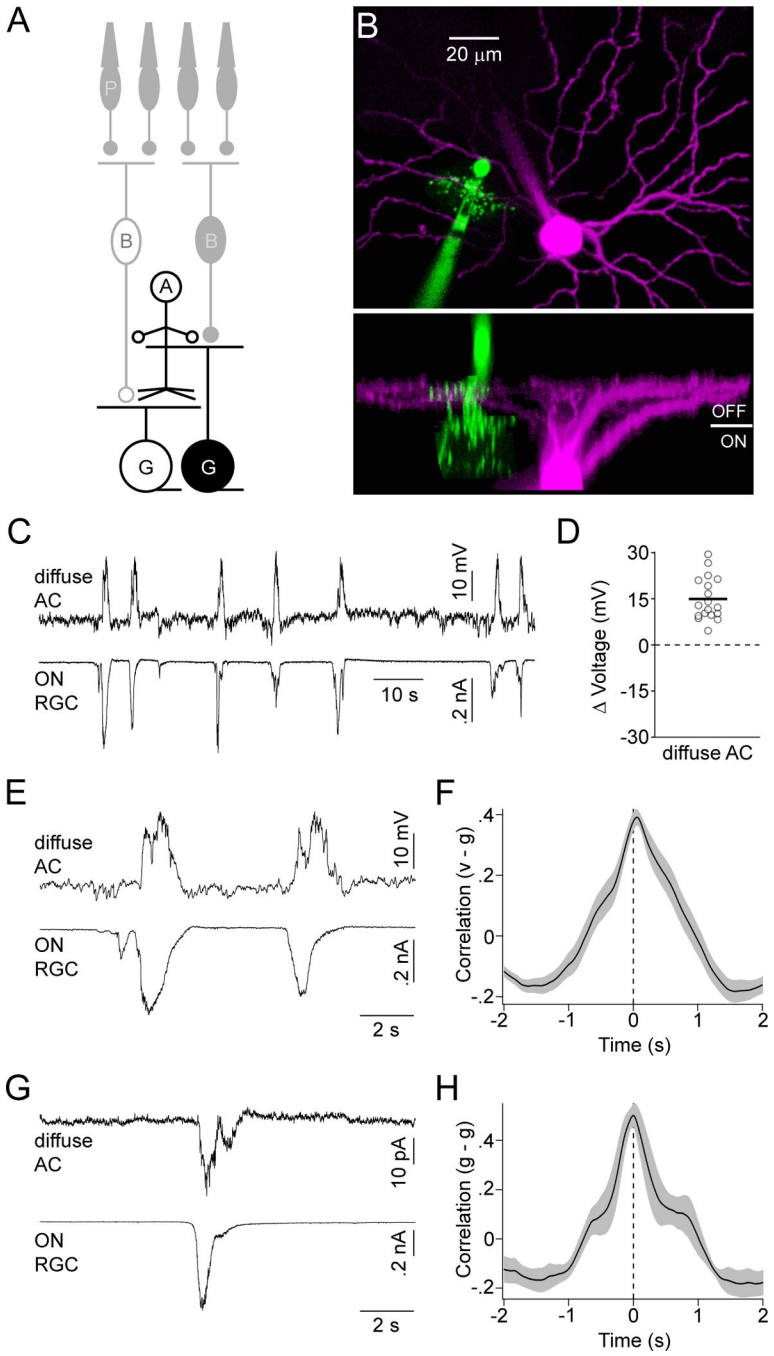

Figure 4. Diffuse ACs receive excitatory input and depolarize during the ON phase of stage III waves

(A) Circuit diagram of the retina in which neurons recorded for this figure are highlighted; labeling as in Figure 1. (B) Orthogonal projections of a 2-photon image stack of a diffuse AC (green) and OFF RGC (magenta) filled during a recording. (C) Simultaneous current- (I = 0 pA, V_{Rest} ~ −46 mV) and voltage-clamp clamp (EPSCs, V_M ~ −60 mV) recording from a diffuse AC and ON RGC, respectively. (D) The mean maximal voltage change during waves for each diffuse AC is indicated by open circles. A solid line shows the mean of all diffuse ACs (n = 18) analyzed. (E) Excerpts of the traces in (C) on an expanded timescale. (F) Crosscorrelation (mean ± SEM, n = 9) of the membrane potential (v) of diffuse ACs

with excitatory conductances in ON RGCs (or inhibitory conductances in OFF RGCs) (g). (G) Simultaneous recording of EPSCs in a diffuse AC and an ON RGC. (H) Crosscorrelation (mean ± SEM, n = 5) of excitatory conductances in diffuse ACs (g) with excitatory conductances in ON RGCs (or inhibitory conductances in OFF RGCs) (g).

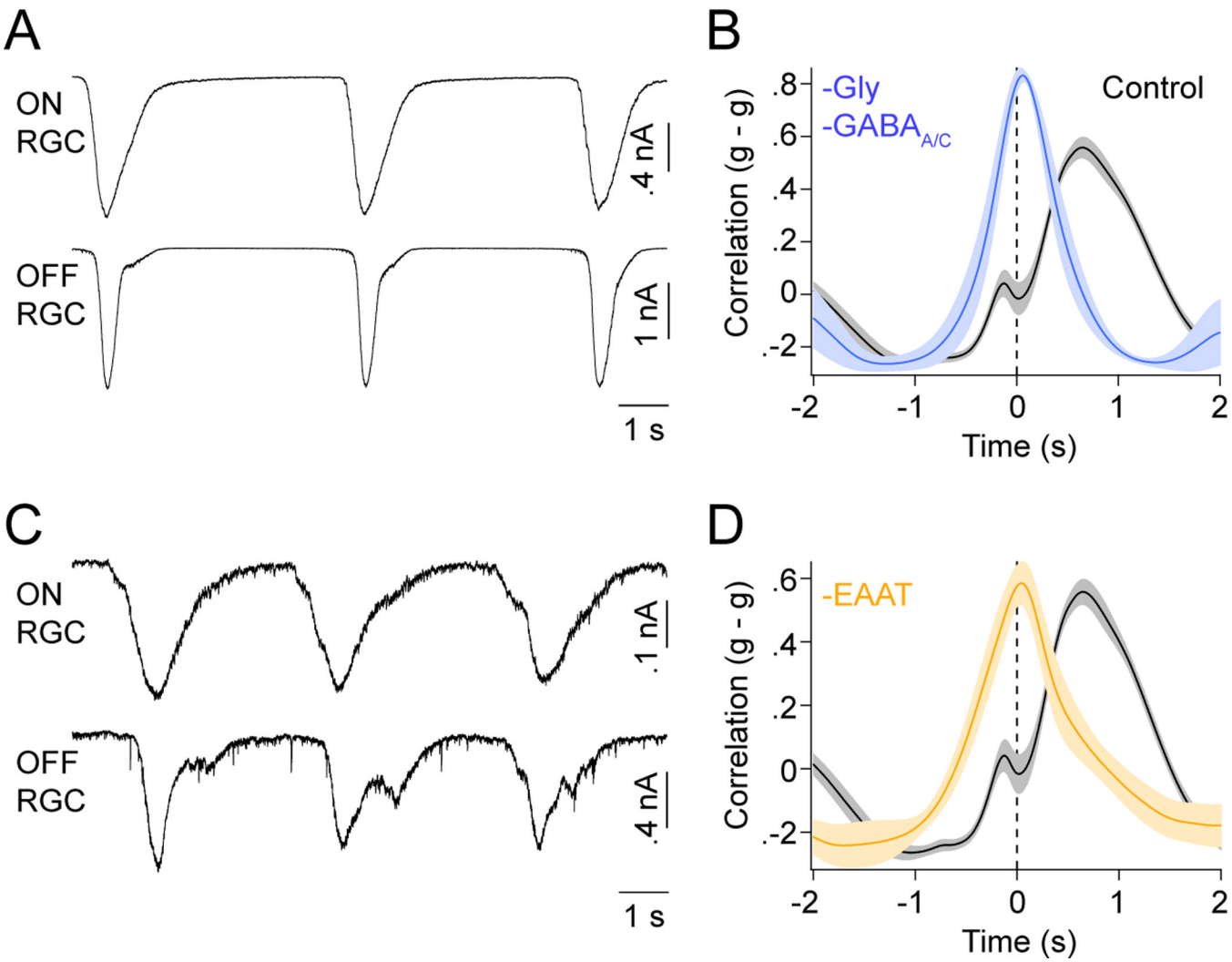

Figure 5. Blockade of crossover inhibition and glutamate uptake synchronize EPSCs of ON and OFF RGCs

(A) Representative simultaneous recording of EPSCs from ON and OFF RGCs in the presence of strychnine (500 nM), gabazine (5 μM) and TPMPA (50 μM). (B) Crosscorrelation (mean ± SEM, Control n = 15, -Gly -GABA$_{A/C}$n = 4) of excitatory synaptic conductances (g) of ON and OFF RGCs in control conditions (black) or in the presence of glycinergic- and GABAergic blockers (blue). (C) Representative EPSC traces from simultaneously recorded ON and OFF RGCs in the presence of the glutamate uptake inhibitor TBOA (25 μM). (D) Crosscorrelation (mean ± SEM, Control n = 15, -TBOA n = 5) of excitatory synaptic conductances in ON and OFF RGCs. As in (B) control results obtained in control conditions are depicted in black. Crosscorrelations recorded in the presence of TBOA are shown in orange. See also Figures S5 and S6.

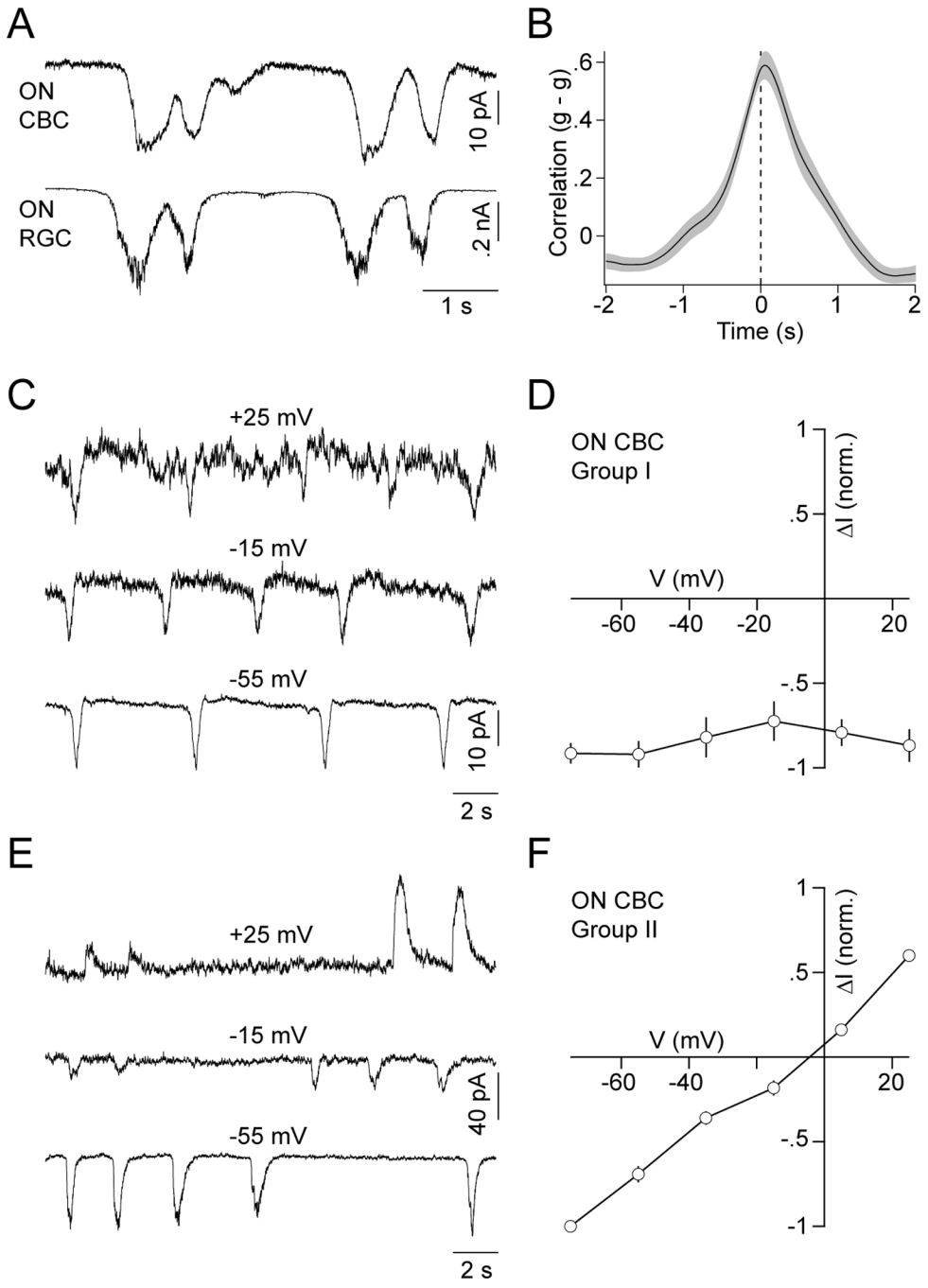

Figure 6. ON CBCs receive excitatory input during waves via cation-nonselctive conductances and gap junctions

(A) Simultaneous recording of EPSCs of an ON CBC and ON RGC during stage III waves. (B) Crosscorrelation (mean ± SEM, n = 8) of excitatory synaptic conductances (g) of ON CBCs and ON RGCs. (C, E) Voltage-clamp traces of a representative group I (C) and II (E) ON CBC in the presence of strychnine (500 nM), gabazine (5 μM) and TPMPA (50 μM) at a series of holding potentials. (D, F) Normalized I-V relationship (mean ± SEM) of wave-associated input currents to group I (D, n = 3) and II (F, n = 3) ON CBCs during blockade of inhibitory synaptic transmission.

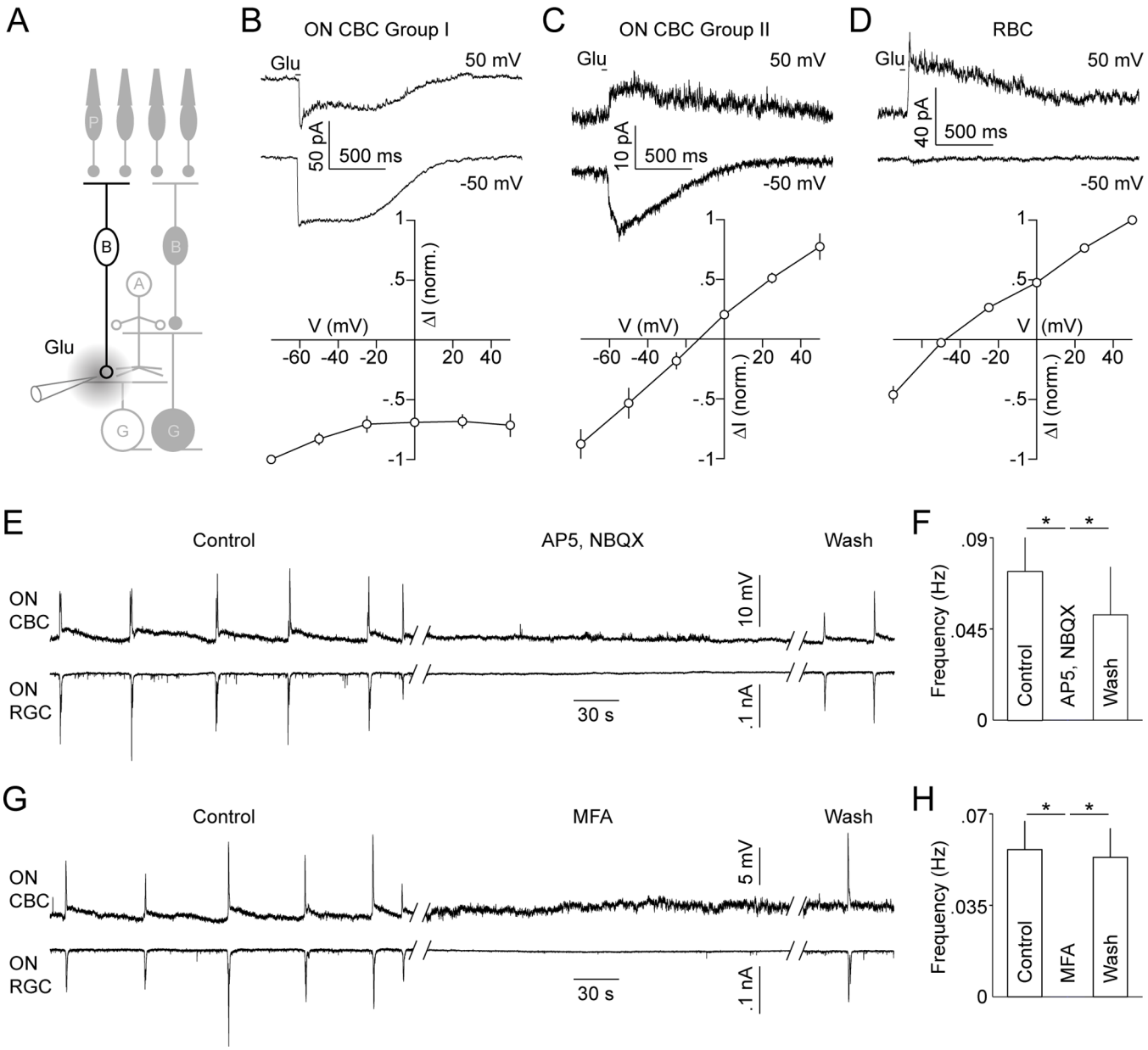

Figure 7. Focal application of glutamate activates distinct currents in ON CBCs and antagonists of iGluRs and gap junctions blocks stage III waves in ON CBCs and RGCs

(A) Schematic illustrating focal application of glutamate in the I PL. (B - D) Representative traces (top panels) and summary data (bottom panels) of currents elicited by glutamate in different BC types: Group I ON CBCs (B, n = 7), group II ON CBCs (C, n = 4) and RBCs (D, n = 5). (E, G) Dual current- (I = 0 pA, V_{Rest} ~ −65 mV) and voltage-clamp (EPSCs, V_M ~ −60 mV) recordings from ON CBCs and ON RGCs, respectively. Traces are shown in control solution, during application of 90 μM AP5 and 20 μM NBQX (E) or 200 μM MFA (G), and after washout of these drugs. (F, H) Average (± SEM) rate of waves in these conditions (AP5, NBQX n = 5; MFA n = 6). See also Figures S7.

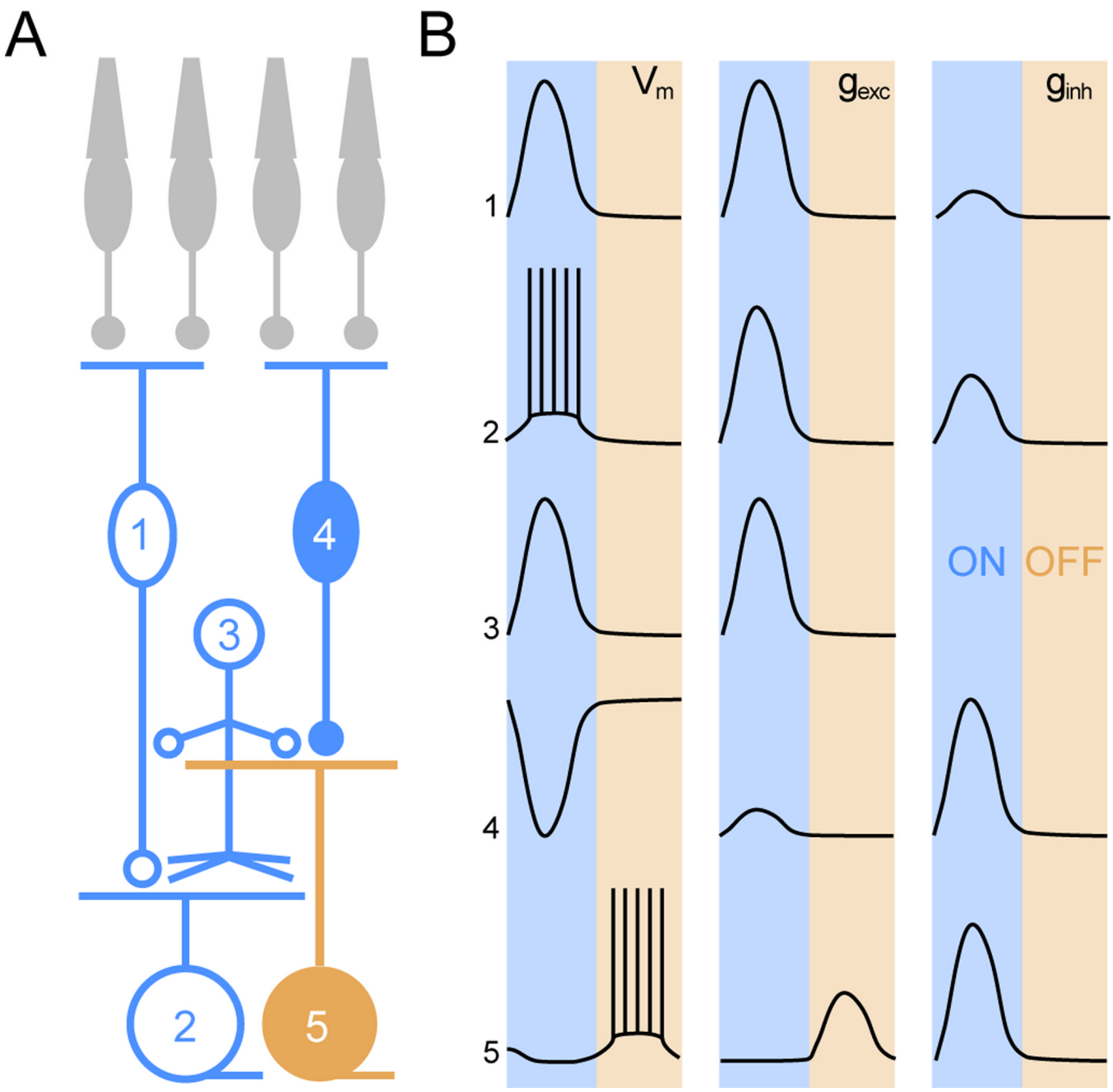

Figure 8. Schematic illustration of retinal circuit activation during stage III waves

(A) Circuit diagram of the retina. Numbers denote: 1 - ON CBC, 2 - ON RGC, 3 - diffuse AC, 4 -OFF CBC, 5 - OFF RGC. Color cording indicates whether the respective neurons participate in the ON (blue) or OFF (orange) phase of stage III waves. (B) Activity patterns (V_M) as well as excitatory (g_{exc}) and inhibitory (g_{inh}) synaptic conductances of the cells depicted in (A) are summarized. Shaded areas mark the ON and OFF phase of stage III waves. The relative amplitudes of g_{exc} and g_{inh} traces are representative of the relative size of these conductances in a given cell but not between different cells.